

# Experimental investigation of downstream wake characteristics of NACA 0015 Airfoil

S. Mano<sup>1</sup>, S. Arunvinthan<sup>1</sup>, and S. Nadaraja Pillai<sup>1,\*</sup>

<sup>1</sup>School of Mechanical Engineering, SASTRA Deemed University, Thanjavur, Tamil Nadu, India.

\*Corresponding author. E-mail: nadarajapillai@mech.sastra.edu

Received: Nov. 19, 2019; Accepted: Feb. 28, 2020

In recent times, air transport has emerged as an important force in driving the globalization process, resulting in an ever increasing passenger growth, which in turn demands reduced in-between timings of preceding flights. One of the prominent factors which influence this in-between timings is the downstream wake characteristics. Therefore, in this current study, a series of wind tunnel investigations were performed to assess the downstream near wake characteristics of the NACA 0015 airfoil at various angles of attack corresponding to  $Re = 1.83 \times 10^5$ . The downstream near wake measurements and turbulence quantities were measured using a Pitot-static probe and a simultaneous pressure scanner, with a sampling frequency of 700Hz. Experimental results revealed the complex nature of the downstream near wake characteristics featuring substantial asymmetry arising out of the incoherent flow separations prevailing over the suction and the pressure side of the airfoil. Aiming at systematically investigating the downstream near wake characteristics, the following parameters like wake width, dissipation length, wake width coefficient, downstream velocity ratio and turbulence intensities were considered in this study. Based on the experimental results, it is found that the wake width and the downstream velocity ratio decreases with the increase in the angle of attack. However, the dissipation length, wake width coefficient and turbulence intensity increase with the increase in the angle of attack. Additionally, attempts were made to understand the physical nature of the near wake characteristics at two and four axial chord downstream locations.

**Keywords:** wake velocity; dissipation length; downstream velocity ratio; wake width coefficient

[http://dx.doi.org/10.6180/jase.202012\\_23\(4\).0004](http://dx.doi.org/10.6180/jase.202012_23(4).0004)

## 1. Introduction

Over the years, due to the increased globalization factors, IATA has estimated that the air passenger numbers might be go doubled by the year 2037 based on 2017 predictions [1]. Hence, the frequency of aircraft operations has to be correspondingly increased to cater the needs of additional passengers. Considering these facts, the frequency of aircrafts taking off and landing at the airports has increased thereby reconstruction that has lead to the in-between timings of taking off and landing. Recent studies suggest that at Hartsfield-Jackson airport, which is considered as the world's busiest airport in Atlanta, Their the frequency of operations is 2 aircrafts per minute [2]. One of the prominent factors which play a vital role in deciding the in-between timings of departure and arrival is the downstream wake

characteristics i.e. wake turbulence induced by the preceding flight is depicted in Fig. 1. Hence the study of wake vortex behavior in the downstream of the aircraft wing becomes quintessential. Spalart et al., [3] discussed about the in-between timings scheduled between the leader and the follower aircrafts and concluded that the downstream wake characteristics exhibit a strong effect on the aerodynamic characteristics of the aircraft wing due to the motion and the persistence of the vortices. Further, Spalart introduced the term, non-dimensional time ( $\tau$ ) which is nothing but the time taken for the decay of the trailing vortices emerging from the airfoil to the freestream atmospheric turbulence level. Following which Kopp et al., [4] and Rudis et al., [5] studied the influence of atmospheric stratifications like time of day, season and latitude etc on the non dimensional

time ( $\tau$ ). Like wise, Lee et al., [6] express another serious concern arising from the downstream wake characteristics of an airfoil about the roof damage on the airport caused by the trailing edge vortices emerging from the airfoil and thus extending to the airport like a small tornado. In order, Garodz and Clawson et al., [7] consolidated that to understand and to validate the complete physics, the flight tests needs to be performed. Even at some earlier researches, according to Garodz et al. [8], smoke canisters were mounted to the tower and various aircraft were flown to mark the location of the vortices. Moreover, later studies suggest that wind tunnel test produce flow fields of good quality and accurate measurements and hence could be possibly used to overcome the cost factor involved with the flight tests. This strategy provides us an opportunity to understand better way of the physical nature of the downstream near wake characteristics using wind tunnel. Likewise, De Bruin et al., [9] experimentally investigated the downstream wake characteristics of the full scale Fokker airliner model in the Duits-Nederlansse wind tunnel (DNW) for various downstream locations. They further investigated the influence of flap positions, engine configurations and landing gear effects on the downstream wake characteristics. Similarly, Hallock et al., [10] claimed that the vortices generated from the wing can be resolved in to streamwise and cross-streamwise components. Cross-streamwise components are believed to be caused by the actuation of control surfaces, wing plan form etc [11]. Therefore, if the wing experiences some changes due to the control surfaces, more than one vortex pair will be generated. Even though, it is a general consensus that the vortex motion is dictated by the ambient atmosphere. Spalart et al., [12] and Gerz and Ehret et al., [13] explored the mechanism behind the decay of the downstream wake and found that, the vorticity of the wake which diffuses slowly into the freestream atmosphere causes "detrainment" which is believed to be the primary reason behind the decay of the wake or reduction in the wake with the increase in the downstream distance. Subsequently, Gerz et al., [14] continued his research and published papers on procedures of predicting the vortex strength and downstream wake parameters. With the advent of highly-sophisticated computers and sensors, the prediction of the downstream wake appears to be quite mature now. Hallock et al., [15] reported that RECAT in the US and the RECAT-EU in the Europe have deployed pulsed Lidar to monitor the vortex behaviour at various airports along the final approach and the initial take off path covering an altitude of up to 1500 feet. Even though the airborne sensors and the meteorological predictive systems combined predictions of the downstream wake characteris-

tics helped understanding the physics of the downstream wake vortices and their parametric changes. Under realistic environments/flow field measurements, a strong enough cross-wind may under predict or over predict the downstream wake characteristics like wake width, dissipation length and turbulence quantities etc. Therefore, the experimental investigation of downstream wake characteristics is still an open area for researchers and the amount of knowledge is still lack.

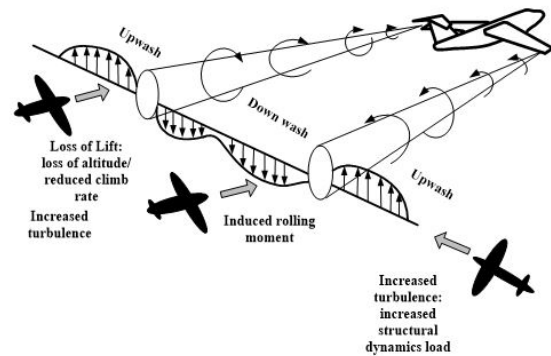


Fig. 1. Wake vortex hazard, Breitsamter et al., [16]

In this context, the present paper deals with a series of wind tunnel experiments aimed at understanding the downstream wake characteristics of the NACA 0015 airfoil subjected to a mean freestream turbulence intensity of 0.51% at  $Re=1.83 \times 10^5$ . The downstream wake measurements were made using the Pitot-static tube and MPS4264 simultaneous pressure scanner of Scanivalve make. The variation of downstream wake parameters like wake width, dissipation length, downstream velocity ratio, wake width coefficient and turbulence quantities were measured for various angles of attack ranging from  $-20^\circ$  to  $20^\circ$ . Additionally, attempts were made to understand the physical nature of the downstream wake characteristics of the test airfoil at two and four axial chord locations respectively. Understanding the wake characteristics downstream of the airfoil will be highly beneficial and could be advantageous for airlines and airport operators to increase the air traffic operations worldwide.

## 2. Experimental setup

An extensive study of aerodynamic characteristics over the symmetrical airfoil was conducted in a low-speed subsonic open-circuit wind tunnel having a rectangular test section of 300 mm 300 mm 1500 mm, as shown in Fig. 2. The test section has a contraction ratio of 3:1, a stable velocity range

of 10 m/s to 60 m/s, and turbulence intensity of 0.51%. The experiments were conducted at Reynolds number ( $Re$ ) =  $1.83 \times 10^5$  with a mean free stream velocity ( $V_\infty$ ) of 28 m/s. The synthesis of the experimental setup is depicted in Fig. 3. A symmetric airfoil model made out of wood with a span length of  $S = 290$  mm and chord length  $C = 100$  mm is utilized in this study. The NACA 0015 based airfoil model was uniformly distributed with 21 pressure taps over the surface of the airfoil. The diameter of each pressure tap was 1mm. The first pressure tap measured the stagnation pressure and the remaining pressure taps measure the surface pressure over the suction side and the pressure side of the airfoil. The test airfoil was mounted horizontally at the centre of the test section using a pitch-position holder. The blockage ratio of the test model is calculated as 4.83%. To characterize the wake profiles at each measurement location, the velocity measurement was performed in a linear translation step size of 10 mm in the  $y$ -direction using Pitot-static tube and simultaneous pressure scanner of Scanivalve make. The downstream measurement locations normalized in terms of chord length were represented as  $(X/C)$ , where  $X$  denotes the distance from the trailing edge of the airfoil to the Pitot-static tube in the  $x$ -direction and  $C$  denoted the chord length between the trailing edge of the airfoil and the Pitot tube. Since the wake behind the test airfoil varied with the increase in the downstream distance and the angle of attack ( $\alpha$ ). Two-downstream measurement locations located at two axial chord lengths ( $2C$ ) and four axial chord lengths ( $4C$ ) in the  $x$ -direction were considered in this study. In addition to the wake measurements, the aerodynamic characteristic of the test airfoil was also studied simultaneously. To measure the instantaneous surface pressure acting over the airfoil the pressure taps from the airfoil were connected to a multichannel pressure scanner. The experiment is carried out for various angles of attack ranging from  $-20^\circ$  to  $20^\circ$  with an increment of  $5^\circ$  at a mean free stream velocity of 28 m/s corresponding to a sampling frequency of 700 Hz and 8,000 data samples. To effectively capture the wake behavior, at each downstream location, the velocities were measured from the bottom to the top of the test section extending between 0 to 300mm with an increment of 10mm in the  $y$ -direction. Based on resultant data, like wake width, dissipation length, effect of downstream velocity ratio, wake width coefficient and turbulence intensity were calculated at velocity at  $V = 28$  m/s ( $Re = 1.83 \times 10^5$ ).

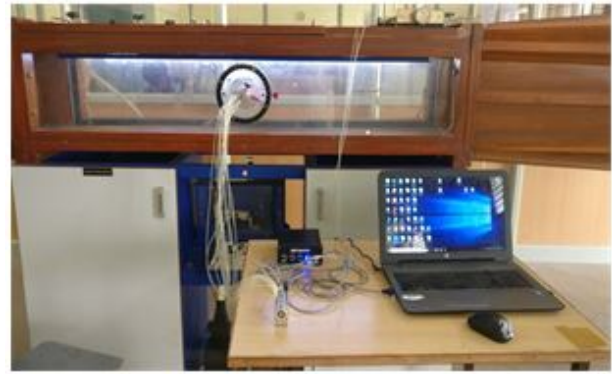


Fig. 2. Experimental setup in a low subsonic wind tunnel

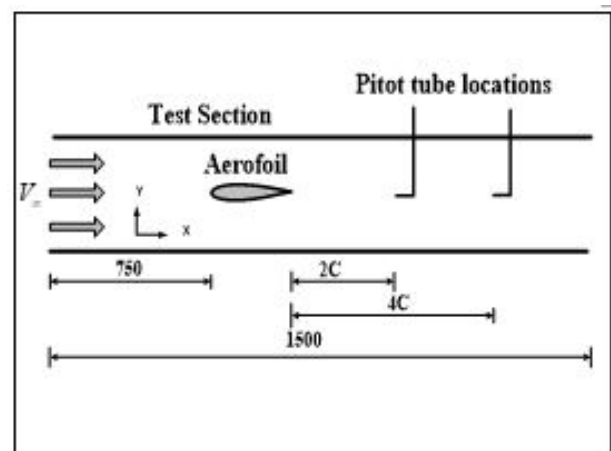


Fig. 3. Pitot location various place at the test section in (mm)

### 3. Result discussions

#### 3.1. Wake velocity measurements

Wake development at downstream was anticipated in schematic outline. In view of this expectation, the test results in downstream wake advancement additionally emulate the same pattern as in Fig. 4. The variation of wake velocity profile with respect to change in angle of attack ( $\alpha$ ) measured at two and four axial chord distances downstream from the trailing edge of the airfoil which is shown in Fig. 5a and Fig. 5b respectively. It is inferred from the Fig. 5a that, broader wakes are formed on the suction side with an increase in angle of attack. At  $\alpha = 20^\circ$ , the wake width shows its maximum peak which is relatively higher than the remaining angles. It is based on the fact that the change in the wake width emerges as a result of the change in the boundary layer followed by the flow separation influenced by the flow velocity and the angle of attack ( $\alpha$ ). Furthermore, with the increase in angle of attack the flow is highly accelerated on the suction side

and decelerated on the pressure side, because of significant flow separation near the trailing edge resulting in broader wake formation as discussed by Zhang et al [17]. From Fig. 5a it can be noted that at lower angles, the wake velocity profile is nearly symmetrical and flow velocity gets separated symmetrically. However, with the increase in angle of attack the trend gradually changes from symmetric to asymmetric influenced by the separation. To further ascertain this behaviour it can be noticed that at the tip wake velocity profile an uninterrupted flow can be observed indicating that the free stream velocity is almost equal to the downstream velocity. Moreover, in the mid-region, the peak behaviour varies with respect to  $y/H$  at every point because the viscous sublayer on the airfoil dominates the inertial sublayer due to the wake turbulence effect. Therefore, it can be concluded that the change in wake velocity is significantly influenced by the separation characteristics of the flow as discussed by Hah.C et al [18]. Fig. 5b represents the variation of wake velocity profile at the fourth axial chord length distance downstream of the airfoil trailing edge. The wake width decreases with an increase in downstream distance as a result of the wake structure becoming more asymmetric. Due to above flow phenomena, velocity defects decreases and so the wake is observed to be wider at  $X/C = 2$  than at  $X/C = 4$  at the same angle of attack. Fig. 6a and Fig. 6b represent the variation of wake width at various the angles of attack for two downstream locations of the airfoil. As it can be seen from the Fig. 6, with an increase in angle of attack the wake width increases. With an increases in the distance of in  $X/C$  downstream locations, the wake velocity profile becomes almost equal to that of the free stream velocity profile.

### 3.2. Effect of downstream velocity ratio $[\theta]$ :

$$\frac{\text{Downstream velocity ratio}[\theta]}{\text{Downstream velocity without the model}[\psi]} = \frac{V_{\phi}}{V_{\psi}} \quad (1)$$

The downstream velocity ratio measurements were estimated at second and fourth axial chord length distance for various angles of attack ranging from  $-20^{\circ}$  to  $20^{\circ}$  are shown in Fig. 7. From the Fig. 7, it becomes clear that the velocity ratio decreases as the  $X/C$  increases. For instance, the downstream velocity ratio at  $\alpha=0^{\circ}$  is 0.95 whereas, with the increase in the angle of attack ( $\alpha$ ), the downstream velocity ratio gradually decreases and reaches a value of 0.70 at  $\alpha=20^{\circ}$ . Similar trend is also observed in the negative direction of angles of attack ( $\alpha$ ). From the aspect of downstream distance i.e.  $X/C$ , it can be observed that for the same angle of attack ( $\alpha$ ), the downstream velocity ratio increases with the increase in the  $x/C$ . The results obtained from the second station indicates that the downstream velocity ratio

increases and reaches 1.05 at  $\alpha = 0^{\circ}$  and decreases to 0.85 at  $\alpha = 20^{\circ}$ .

### 3.3. Effect of Wake width co-efficient

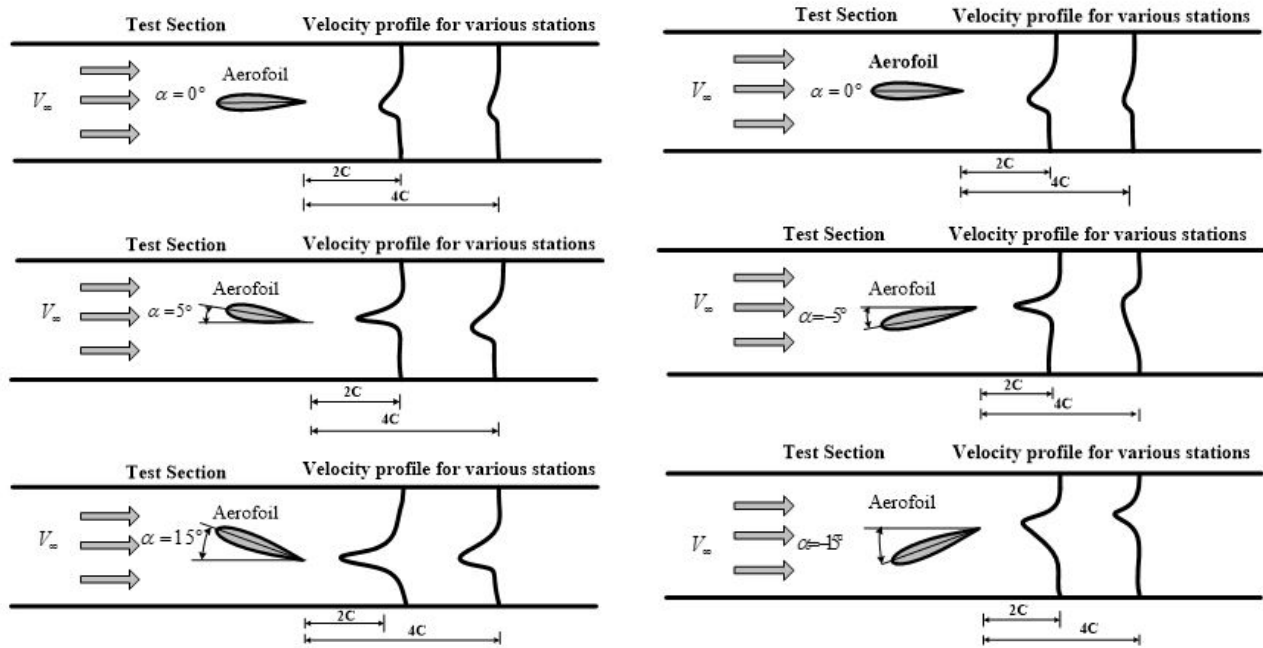
The wake width coefficient is defined as the ratio between dissipation length ( $\Phi$ ) and wake width ( $\delta$ ). Fig. 8a represents the schematic diagram of wake width ( $\delta$ ) and dissipation length for various downstream locations. It is based on the fact that, with the increase in the downstream distance  $X/C$ , the wake width gradually decreases and becomes almost equal to that of the freestream velocity [19]. Further, it can also be seen that with the increase in the downstream distance and decrease in the wake width the dissipation length expands gradually towards the farthest point. Based on the experimental results, it is observed that the wake width coefficient increases with the increase in the angle of attack for both the positive and negative direction of angles of attack. For instance, at  $X/C = 2$ , the wake width coefficient exhibits a value of 0.15 at  $\alpha = 0^{\circ}$ . However, at  $\alpha = 20^{\circ}$ , the wake width coefficient reaches a maximum value of 0.6. The increasing trend of the wake width coefficient with the increase in the angle of attack could be possibly attributed to the reduction in the wake width experienced by the airfoils at higher angles of attack. A similar trend can also be seen for the downstream location  $X/C=4$ , where the wake width coefficient increases from 0.1 at  $\alpha = 0^{\circ}$  to 0.5 at  $\alpha = 20^{\circ}$ .

### 3.4. Turbulent intensity of wake

Since the airfoils subjected to various angles of attack undergo different flow characteristics, the downstream wake of the airfoil over the pressure and the suction side is relatively different featuring substantial asymmetry. To further identify the influence of downstream wake characteristics on the turbulence quantities of the flow field, turbulence intensity distribution across various angles of attack at  $X/C = 2$  and 4 is plotted in fig. 9a and 9b respectively. Figure 9a and 9b shows that the level of turbulence intensity is higher on the suction side relative to the pressure side at both the downstream locations. However, it can be further inferred that with the increase in the angle of attack the wake characteristics of an airfoil exhibits a significant effect on the turbulence quantities of the flow field. For instance, it could be easily seen from the figure that, for  $\alpha < 10^{\circ}$  a noticeable change in the level of turbulence intensity is observed.

## 4. Conclusions

The downstream characteristics of NACA 0015 airfoil has been studied at various locations with the parameters like



(a) Wake velocity development in positive AOA

(b) Wake velocity development in negative AOA

**Fig. 4.** Schematic diagram of the velocity profile represents the wake development in various downstream locations along the x-direction.

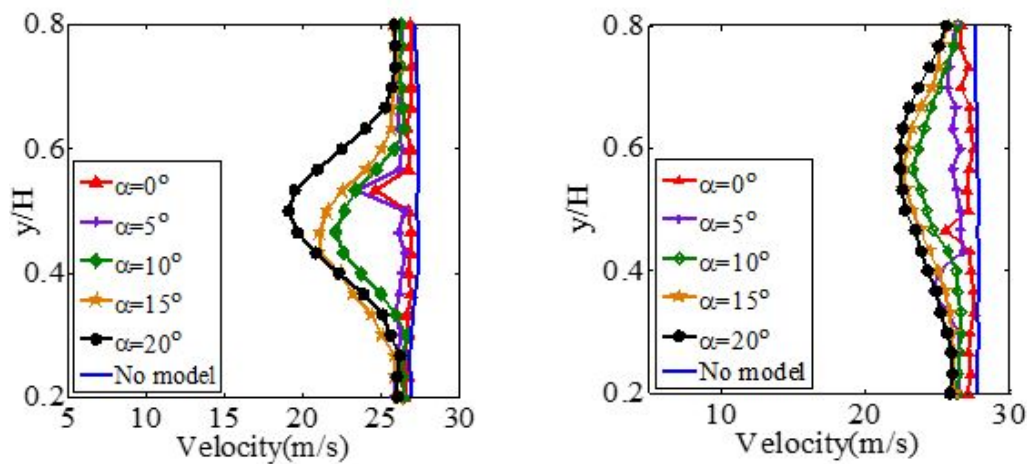


**Fig. 5.** (a) Wake velocity profile at  $X/C = 2$ . (b) Wake velocity profile at  $X/C = 4$ .

wake width, dissipation length, wake width ratio and downstream velocity ratio. Based on the experimental data the following conclusions were made.

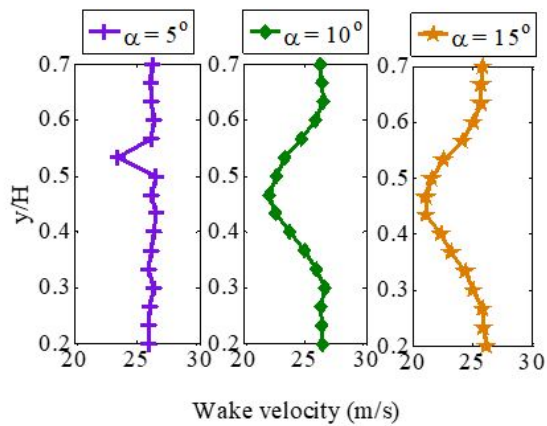
I. The wake width increases with an increase in angle of attack and decreases with an increase in downstream distance for the same angle of attack. The dissipation length increases with an increase in angle of attack and also increase with increasing in downstream distance.

II. with the increase in positive angle of attack, asym-

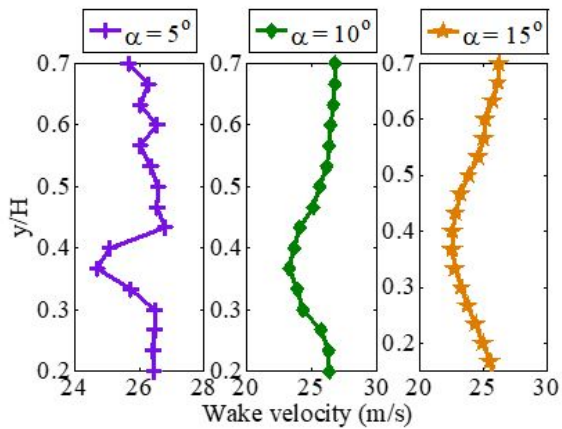
metric nature of wake increases and moves towards the negative y-direction. The opposite behavior is observed for the negative angle of attack.

III. Downstream velocity ratio increases with an increase in downstream distance for the same angle of attack and far from the trailing edge of airfoil it will be equal to free stream velocity.

IV. Wake width coefficient decreases with an increase in angle of attack and it increases with increasing downstream



(a)



(b)

**Fig. 6.** (a) Mean velocity profile at station  $X/C = 2$  for angle  $\alpha = 5^\circ, 10^\circ$  and  $15^\circ$ . (b) Mean velocity profile at station  $X/C = 4$  for angle  $\alpha = 5^\circ, 10^\circ$  and  $15^\circ$

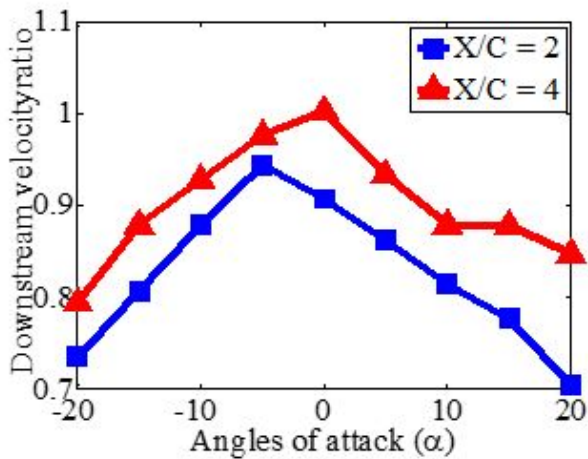
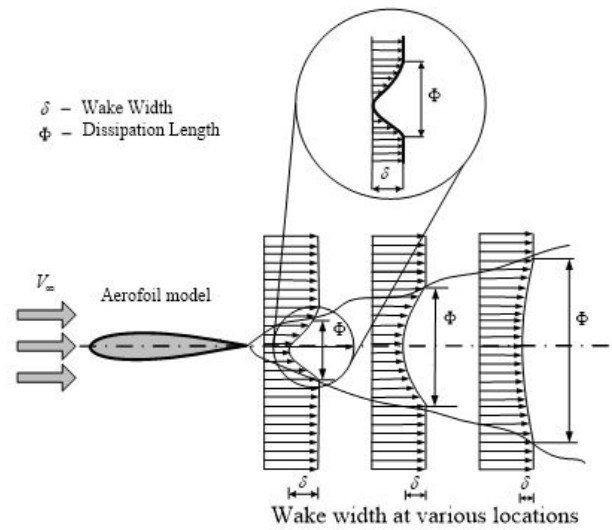
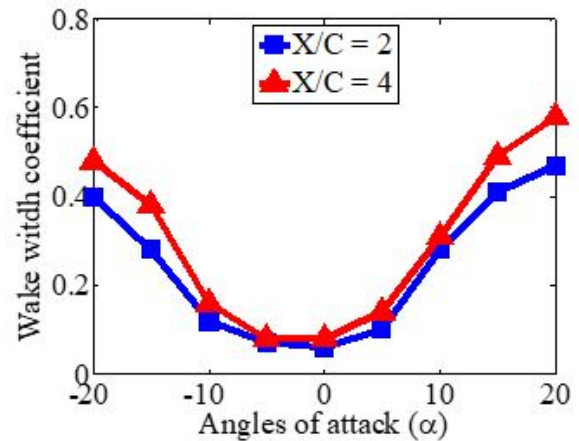


**Fig. 7.** Downstream velocity ratio  $[\theta]$  for the various angles of attack.



(a)



(b)

**Fig. 8.** (a) Wake velocity development in positive AOA. (b) Wake velocity development in negative AOA.

distance. The investigation was performed in such a way that measurements were limited to a downstream length of  $4C$ .

**Acknowledgements**

This work was supported by the “Research and Modernization fund, SASTRA Deemed to be University” grant number R&M/0035/SoME-008/2015-16. The authors thank SASTRA Deemed to be University for their financial assistance in performing an aerodynamic investigation of surface pressure and downstream characteristics of the symmetrical airfoil.

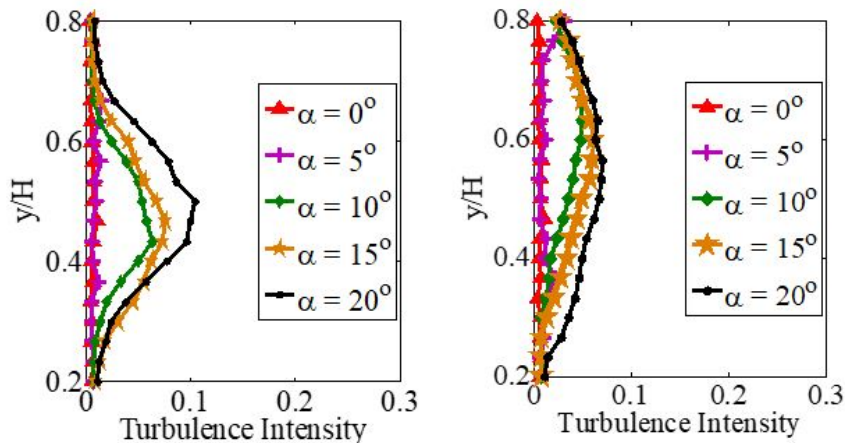


Fig. 9. (a) Turbulence intensity at  $X/C = 2$ . (b) Turbulence intensity at  $X/C = 4$ .

## References

- [1] IATA report based on 2017 data.
- [2] Tony Diana. An evaluation of departure throughputs before and after the implementation of wake vortex recategorization at Atlanta Hartsfield/Jackson International Airport: A Markov regime-switching approach. *Transportation Research Part E: Logistics and Transportation Review*, 83:216–224, 2015.
- [3] Philippe R. Spalart. AIRPLANE TRAILING VORTICES. *Annual Review of Fluid Mechanics*, 30(1):107–138, jan 1998.
- [4] Friedrich Köpp. Doppler lidar investigation of wake vortex transport between closely spaced parallel runways. *AIAA Journal*, 32(4):805–810, 1994.
- [5] RP Rudis, DC Burnham, and P Janota. *Wake vortex decay near the ground under conditions of strong stratification and wind shear*. 1996.
- [6] G. H. LEE. Trailing vortex wakes. *Aeronaut. J.*, 79(377), 1975.
- [7] Clawson KL Garodz LJ. Vortex wake characteristics of B757- 200 and B767-200 aircraft using the tower fly by technique. Technical report, 1993.
- [8] Leo J Garodz, David M Lawrence, and Nelson J Miller. Measurement of the trailing vortex systems of large transport aircraft, using tower fly-by and flow visualization (summary, comparison and application). Technical report, 1974.
- [9] Anton C De Bruin, G H Hegen, P B Rohne, and Ph R Spalart. Flow field survey in trailing vortex system behind a civil aircraft model at high lift. In *AGARD CONFERENCE PROCEEDINGS AGARD CP*, pages 25–25, Trondheim, Norway, 1996.
- [10] J N Hallock and John A Volpe. Aircraft Wake Vortices: An Assessment of the Current Situation. Technical Report January 1991, 1991.
- [11] Lung Jieh Yang, Cheng Kuei Hsu, Hsieh Cheng Han, and Jr Ming Miao. Light flapping micro aerial vehicle using electrical-discharge wire-cutting technique. *Journal of Aircraft*, 46(6):1866–1874, 2009.
- [12] PR Spalart and AA Wray. Initiation of the Crow instability by atmospheric turbulence. Technical report, Trondheim, Norway, 1996.
- [13] T Gerz and T Ehret. Wake dynamics and exhaust distribution behind cruising aircraft. Technical report, Trondheim, Norway, 1996.
- [14] Thomas Gerz, Frank Holzäpfel, and Denis Darracq. Commercial aircraft wake vortices, apr 2002.
- [15] James N. Hallock, George C. Greene, and David C. Burnham. Wake Vortex Research—A Retrospective Look. *Air Traffic Control Quarterly*, 6(3):161–178, jul 1998.
- [16] C. Breitsamter. Wake vortex characteristics of transport aircraft, 2011.
- [17] Wei Zhang, Wan Cheng, Wei Gao, Adnan Qamar, and Ravi Samtaney. Geometrical effects on the airfoil flow separation and transition. *Computers and Fluids*, 116:60–73, aug 2015.
- [18] C Hah and B Lakshminarayana. Measurement and prediction of mean velocity and turbulence structure in the near wake of an airfoil. *Journal of Fluid Mechanics*, 115:251–282, 1982.
- [19] G. Balaji, S. Nadaraja Pillai, and C. Senthil Kumar. Wind tunnel investigation of downstream wake characteristics on circular cylinder with various taper ratios. *Journal of Applied Fluid Mechanics*, 10(SpecialIssue):69–77, 2017.